Title

Risk assessment of cardiotoxicity to zebrafish (Danio rerio) by environmental exposure to triclosan and its derivatives

Journal

Environmental Pollution, 265(Pt A)

ISSN

0269-7491

Authors

Wang, Danting
Zhang, Yuhuan
Li, Jieyi
et al.

Publication Date

2020-10-01

DOI

10.1016/j.envpol.2020.114995

Peer reviewed

Environmental Pollution 265 (2020) 114995

Contents lists available at ScienceDirect

Environmental Pollution

journal homepage: www.elsevier.com/locate/envpol

Risk assessment of cardiotoxicity to zebrafish (*Danio rerio*) by environmental exposure to triclosan and its derivatives☆

Danting Wang [a], Yuhuan Zhang [a], Jieyi Li [a], Randy A. Dahlgren [b], Xuedong Wang [c], Haishan Huang [a], Huili Wang [a, *]

[a] Zhejiang Provincial Key Laboratory of Medical Genetics, Key Laboratory of Laboratory Medicine, Ministry of Education, School of Laboratory Medicine and Life Sciences, Wenzhou Medical University, Wenzhou, Zhejiang, 325035, China
[b] Department of Land, Air and Water Resources, University of California, Davis, CA, 95616, USA
[c] National and Local Joint Engineering Laboratory of Municipal Sewage Resource Utilization Technology, School of Environmental Science and Engineering, Suzhou University of Science and Technology, Suzhou, Jiangsu, 215009, China

ARTICLE INFO

Article history:
Received 4 March 2020
Received in revised form
2 June 2020
Accepted 6 June 2020
Available online 10 June 2020

Keywords:
Triclosan
Environmental toxicology
Zebrafish
Cardiac marker gene
KEGG pathway

ABSTRACT

Triclosan (TCS) and its two derivatives (2,4-dichlorophenol and 2,4,6-trichlorophenol) are priority pollutants that coexist in aquatic environments. Joint exposure of TCS, 2,4-dichlorophenol and 2,4,6-trichlorophenol, hereafter referred to as TCS-DT, contributes severe toxicity to aquatic organisms. There is currently a paucity of data regarding TCS-DT molecular toxicity, especially on cardiac diseases. We used zebrafish (*Danio rerio*) as a model organism, and evaluated the molecular-level cardiotoxicity induced by TCS-DT from embryonic to adult stages. TCS-DT exposure prominently led to phenotypic malformations, such as pericardial cysts, cardiac bleeding, increased SV-BA distance, decreased heart rate and reduced ejection fraction, as well as abnormal swimming behavior. Analyses of the GO and KEGG pathways revealed enrichment pathways related to cardiac development and screened for significantly down-regulated adrenaline signaling in cardiomyocytes. The cardiac marker genes (*amhc*, *cmlc2*, *vmhc*, and *nkx2.5*) were obtained through protein-protein interaction (PPI) networks, and expressed as down-regulation by WISH. After chronic exposure to TCS-DT from 30 to 90-dpf, both body mass and heart indexes prominently increased, showing myocardial hypertrophy, abnormal heart rate and histopathological injury. Heart tissue damage included disordered and ruptured myocardial fibers, broken and dissolved myofilaments, nuclear pyknosis, mitochondrial injury and inflammatory cell infiltration. Further, abnormal changes in a series of cardiac functions-related biomarkers, including superoxide dismutase, triglyceride, lactate dehydrogenase and creatinine kinase MB, provided evidence for cardiac pathological responses. These results highlight the molecular mechanisms involving TCS-DT induced cardiac toxicity, and provide theoretical data to guide prevention and treatment of pollutant-induced cardiac diseases.

1. Introduction

Triclosan (TCS) is widely used in medical and personal care products owing to its broad-spectrum antibacterial effect (Dann and Hontela, 2011). However, it may pose serious health risk to human, wildlife and aquatic organisms (Olaniyan et al., 2016). TCS levels in human tissues, urine, blood, and breast milk had been reported to be related to the usage of this antimicrobial agent (Ruszkiewicz et al., 2017); for example, it was even detected in the range of 2.3–3620 μg/L in approximately 80% of urine samples in the USA population (Adgent and Rogan, 2015). Although TCS is a stable and lipophilic compound, it can be transformed into more toxic and bioaccumulative derivatives once in the aquatic environment (Morales et al., 2005), namely 2,4-dichlorophenol (2,4-DCP) and 2,4,6-trichlorophenol (2,4,6-TCP). These intermediates are by-products of water chlorination and combustion processes, contributing to their widespread occurrence in the environment (Jin et al., 2012). Both 2,4-DCP and 2,4,6-TCP are classified as highly carcinogenic chemicals, and thus treated as priority pollutants by many countries (Du et al., 2016; Jiang et al., 2015). TCS and its main

☆ This paper has been recommended for acceptance by Dr. Sarah Harmon.
* Corresponding author.
E-mail address: whuili@163.com (H. Wang).

https://doi.org/10.1016/j.envpol.2020.114995
0269-7491/

derivatives were frequently detected in soil and municipal sewage at the level of ng/L-μg/L. They cause high bioaccumulation not only in the human body, but also in aquatic organisms such as fish and shellfish (Wang and Tian, 2015; Meador et al., 2018; Lu et al., 2019). In 15 European countries, the concentrations of TCS in effluents of sewage treatment plants reached up to 47800 ng/L (Thomaidi et al., 2017). In China surface water, 2,4-DCP (1.1–19960 ng/L) and 2,4,6-TCP (1.4–28650 ng/L) were detected in the Yellow River, Huaihe and Haihe River watersheds (Gao et al., 2008). In the surface water of Taihu Lake, the concentrations of 2,4-DCP ranged from 0 to 143 ng/L, while those of 2,4,6-TCP varied between 0 and 840 ng/L (Zhong et al., 2010).

Chronic TCS exposure may cause biological genotoxicity, hepatotoxicity, immunotoxicity, neurotoxicity and cardiotoxicity, as well as impairment of lipid metabolism (Ho et al., 2016; Yueh and Tukey, 2016). TCS leads to craniofacial morphosis in zebrafish (Kim et al., 2018), and acute TCS exposure induces subtle cardiotoxicity in developing fish (Saley et al., 2016). Also, TCS results in changes in fertility function in different animal models. Exposure of pregnant rats and mice to TCS can impair placental development and nutritional transfer (Feng et al., 2016; Cao et al., 2017). In addition to leading to reproductive toxicity in the *Caenorhabditis elegans* (0.1–2 mg/L), oxidative stress and endocrine disruption have been reported due to TCS exposure (Lenz et al., 2017). 2,4-DCP (60–960 μg/L) and 2,4,6-TCP (50–800 μg/L) contribute to oxidative stress in freshwater bivalves (Xia et al., 2016). 2,4-DCP had been reported to significantly reduce heart rate with increased exposure concentration (Li et al., 2018). 2,4-DCP and 2,4,6-TCP were further hypothesized to lead to obesity and dyslipidemia (Parastar et al., 2018). Importantly, TCS, 2,4-DCP and 2,4,6-TCP coexist in real-world aquatic environments, creating the potential for synergistic toxicity interactions (Tixier et al., 2002; Bedoux et al., 2011). Meanwhile, we used zebrafish (*Danio rerio*) as a model organism, which has unique advantages in heart development research, such as high-resolution imaging of whole heart, clear heart development process and early development process as similar as human. Therefore, it is called “the research window of heart development” (Sarmah and Marrs, 2016). Besides, zebrafish maintain their ability to regenerate heart tissue throughout their life (Poss et al., 2002).

Our previous work revealed that TCS-DT decreased zebrafish hatching rate, and led to a series of malformations, such as cardiovascular malformation and fat-metabolism disorder (Lin et al., 2017; Liu et al., 2018; Zhang et al., 2018). However, the role of TCS-DT exposure in inducing cardiotoxicity to aquatic organisms require further rigorous investigation to address the related molecular mechanisms. Based on the prevalence of TCS-DT induced phenotype malformations, we performed a series of experiments to examine the molecular pathways of TCS-DT exposure on zebrafish, such as high throughput RNA-seq and signaling pathway analyses on heart development deficit by protein-protein interaction (PPI) networks. We screened four cardiac marker genes (*amhc, cmlc2, vmhc* and *nkx2.5*) to evaluate whether their expression changed with acute TCS-DT exposure using qRT-PCR and whole-mount in-situ hybridization (WISH) techniques. Cardiac malformations were observed by Masson’s trichrome staining, Haematoxylin and Eosin (H&E) staining and transmission electron microscopy (TEM) following chronic TCS-DT exposure. Zebrafish cardiotoxicity, induced by chronic TCS-DT exposure, revealed molecular-level responses, from embryonic development to adult cardiac function. Overall, these results provide a systematic approach for evaluating the joint cardiotoxicity of chlorinated phenolic pollutants in aquatic environments.

2. Materials and methods

2.1. Ethics statement

Our zebrafish-use protocols were approved by the Institutional Animal Care & Use Committee (IACUC) at Wenzhou Medical University. We conducted all experiments in strict compliance with IACUC guidelines. Dissection was performed on ice to minimize zebrafish suffering.

2.2. Chemicals reagents

TCS, 2,4,6-TCP and 2,4-DCP (chemical purity $\geq$ 98.0%) were acquired from Sigma-Aldrich (St. Louis, USA), and their CAS No. and purities were summarized in Table S1. The stock solutions of three chemicals were prepared in acetone and stored at −20 °C for use. The mixture of TCS, 2,4-DCP and 2,4,6-TCP is hereafter referred to as TCS-DT.

2.3. Zebrafish maintenance and exposure protocols

Wild-type (AB strain) zebrafish maintenance followed previously reported protocols (Li et al., 2016). Our previous study determined LC_{50} and EC_{50} values for TCS-DT of 2.28 and 1.16 mg/L, respectively. TCS-DT exposure concentrations were based on the 1/8 to 1/3 increments of the LC_{50} value (Liu et al., 2018; Zhang et al., 2018) resulting in four TCS-DT concentrations (0, 0.28, 0.56 and 0.84 mg/L) for 6–120 h post-fertilization (hpf) zebrafish embryo exposure. Control group included 0.0084% acetone, which was referred to the highest 0.84 mg/L TCS-DT-exposure treatment. This study referred to the optimal concentration ratio of TCS, 2,4,6-TCP and 2,4-DCP (1: 2: 4) for evaluation (Zhang et al., 2018), and their individual concentrations in each concentration of TCS-DT are listed in Table S1. In the control group and 0.84 mg/L TCS-DT-exposure treatment group, 100 larval zebrafish at 120-hpf were employed for extracting the RNA-seq sample for each replicate, and each group was composed of two biological replicates ($n = 2$). As a consequence, a total of 400 larvae were used for four RNA-seq samples. Additionally, adult zebrafish were exposed to TCS-DT concentrations of 0, 0.14, 0.28 and 0.56 mg/L from 30 to 90 days post-fertilization (dpf). These nominal (fortified) TCS-DT-exposure concentrations simulated real-world environmental levels in aquatic ecosystems. In order to maintain stable water quality and TCS-DT concentration, the exposure solution was renewed daily (6–120 hpf and 30–90 dpf). A schematic representation of overall experimental design is depicted in Fig. S1.

2.4. Assessment of TCS-DT-induced cardiotoxicity

To evaluate the effects of TCS-DT exposure on larval heart development, we assessed cardiac malformations, including heart rate, ejection fraction and SV-BA distance.

(i) Heart rate and ejection fraction measurements

Subsequent to exposure to TCS-DT from 6 hpf, we observed the 48-hpf embryos using a stereoscope coupled to a digital camera (SZX16, Olympus, Japan) to record video images for determination of heartbeat rate for 2 min at 28.5 °C (Li et al., 2019). We used area subtraction to estimate ejection fraction according to Matrone and coworkers’ report (Matrone et al., 2014). Briefly, the ventricular contraction area was substracted from the diastolic area of the heart, which were expressed as a percentage of the diastolic area.

(ii) SV-BA distance measurement

After TCS-DT exposure, changes in larval cardiac morphology were detected by acquiring lateral images to determine the SV-BA distance between sinus venous (SV) and balloon arterial (BA). Imaging software was utilized to compute the length of lines connecting the two structures on the acquired images (Antkiewicz et al., 2005).

2.5. Behavioral assessment

In this study, 120-hpf zebrafish larvae were transferred to 96-well plates and placed directly in the DanioVision Observation Chamber (Noldus IT, Wageningen, Netherlands) to evaluate the larval responses to external stimuli and spontaneous movements (without any irritation). Zebrafish were preadapted for 5 min prior to light stimulation. In the light-dark stimulation process, we used video analysis to determine average swim distance using EthoVision XT software (Noldus IT).

2.6. Illumina mRNA-seq and bioinformatics analysis

We extracted total RNA using Trizol Reagent (Invitrogen, CA, USA). Bioanalyzer 2100 and RNA 1000 Nano Lab Chip Kit (Agilent, CA, USA) were used to detect the quantity and purity of total RNA, and the RIN number $\geq$ 9.6, respectively. Poly(A) RNA was purified from total RNA (5 μg) using poly-T oligo-attached magnetic beads. After two rounds of purification, the divalent cations were used to fragment the mRNA into small pieces under elevated temperature. Subsequently, the final cDNA library was created by reverse transcription of the cleaved RNA fragments. The detailed procedures were carried out according to the mRNA-Seq sample preparation kit (Illumina, San Diego, USA), and the average insert size for the paired-end library was 300 bp (±50 bp). Paired-end sequencing performed using an Illumina_HiSeq4000 (LC Sciences, Houston, USA) followed the vendor's recommended protocols (Mortazavi et al., 2008; Wang et al., 2012). We used StringTie to analyze the expression levels of mRNAs by calculating Fragments Per Kilobase per Million (FPKM) (Trapnell et al., 2010). Differentially expressed mRNAs/genes were screened on the basis of $\log_2$(fold change) > 0.5 or < -0.5 at $p < 0.05$ using Feature Count software (Liao et al., 2014). Functional annotation of differentially expressed genes (DEG) was conducted by Gene Ontology (GO) (http://www.geneontology.org/) and "Kyoto Encyclopedia of Genes and Genomes" (KEGG) (http://www.genome.jp/kegg/) functional classification (Kanehisa et al., 2007; Young et al., 2010) and Database for Annotation, Visualization and Integrated Discovery (DAVID, http://david.abcc.ncifcrf.gov/)(Huang et al., 2008). We imported each protein list encoded by DEGs into the "Search Tool for Retrieving Interacting Genes" (STRING 11.0) database (http://string-db.org/) for the sake of building a PPI network. We used Cytoscape 3.6.1 software (http://www.cytoscape.org/) to map the protein-protein interaction (PPI) network and pathway localization of genes involved in cardiac development.

2.7. qRT-PCR and WISH for heart-related genes

We performed qRT-PCR and WISH to evaluate the genes related to heart development. When exposed to TCS-DT from 6 to 120 hpf, total RNA of 50 larval zebrafish homogenized for each replicate of different groups (0, 0.28, 0.56 and 0.84 mg/L) was isolated using TRIzol reagent, and *elfa* and *β-actin* were used as the endogenous reference (McCurley and Callard, 2008). The primers for qRT-PCR are listed in Tables S2–S3. The cDNA probe sequences of four genes (*amhc*, *cmlc2*, *vmhc* and *nkx2.5*) in WISH were labeled with digoxigenin (DIG) (Fig. S2). The 6-hpf embryos were exposed to TCS-DT (0, 0.28, 0.56 and 0.84 mg/L), and the control and treatment groups were treated with 0.5% N-phenylthiourea (PTU, Aladdin, Shanghai, China). The 24, 48 and 72-hpf larvae were collected for WISH (Thisse and Thisse, 2008) and the results recorded using a microscope camera (SZX16, Olympus, Japan). Each group was performed in triplicate, and the primers for WISH are listed in Table S4.

2.8. Measurements of TG, LDH, CK-MB and SOD

We recorded myocardial cellular damage by measuring triglyceride (TG), lactate dehydrogenase (LDH) and creatinine kinase MB (CK-MB) levels in heart tissue using a fully automated biochemical analyzer and a commercial assay kit (Rayto, Shenzhen, China). Superoxide dismutase (SOD) activity is an indicator of reactive oxygen radical and lipid superoxide levels (Lubrano and Balzan, 2015), which was detected in the 90-dpf adult heart using the hydroxylamine method (Nanjing Jiancheng Bioengineering Institute, Nanjing, China).

2.9. Histopathological observation of heart tissue

After TCS-DT exposure from 30 to 90 dpf, zebrafish heart tissue was dissected for histopathological observation. We performed H&E staining of the isolated heart tissue using a HE®Staining kit (Solarbio, Beijing, China) following manufacturer's instructions. Paraffin sections (4 μm) were Masson stained to differentiate between normal and diseased heart tissues; muscle fibers were red and collagen fibers were blue. Microscopic observation of heart damage was assessed using transmission electron microscopy (TEM7500, Hitachi, Tokyo, Japan).

2.10. Statistical analysis

Experimental data are reported as the mean ± standard deviation (SD). Table S5 summaries the number of biological replicates, technological replicates and zebrafish evaluated at different developmental stages. We assessed the TCS-DT treatment effects using one-way analysis of variance (ANOVA). All statistical analyses were conducted with SPSS 18.0 (SPSS, Chicago, USA) using $p < 0.05$ (*), $p < 0.01$ (**) or $p < 0.001$ (***) significance levels, unless otherwise stated.

3. Results

3.1. Effects of TCS-DT exposure on zebrafish morphology and swimming behavior

Three TCS-DT concentrations were implemented to evaluate the exposure effects on cardiac development and swim behavior. Prominent heart phenotypic defects occurred for 72-hpf larvae with a dose-response relationship. The 0.28 mg/L treatment produced a slight pericardial cyst (PC), and the 0.56 mg/L treatment resulted in severe yolk retention, PC, and SV bleeding. In the 0.84 mg/L treatment, dysplasia became more pronounced, which included small eye deformities, yolk cyst, severe PC, SV bleeding, closure of swim sac (SS), ear capsule and otolith differentiation defects (Fig. S3A).

The standard for assessing whether hearing and vision are developing normally is the stress response of zebrafish larvae to external sound or optical stimuli (Einhorn et al., 2012). Average swim distance after stimulation served as a response sensitivity and vitality metric. There was a slight increase in spontaneous movement distance for embryos in the 0.28 and 0.84 mg/L treatments at 24-hpf (fetal movement) ($p > 0.05$). In contrast, the 0.56 mg/L TCS-DT treatment produced a significant increase ($p < 0.05$) in spontaneous movement distance (Fig. S3B). Light-dark

rhythm activities of 120-hpf larvae were evaluated using a 30-min alternating photoperiod stimulation (Chen and Wang, 2012). In the control group, larval swim activity showed an initial burst after a rapid transition from dark-to-light; followed by regular motion rhythms consisting of more exercise during dark conditions and less exercise in light conditions. In contrast, the 0.28 mg/L treatment yielded excessive excitement, although there were also regular reaction rhythms to light-dark stimulation. Finally, the 0.56 and 0.84 mg/L treatments resulted in insensitive responses to light-dark stimulation (Fig. S3C).

3.2. Heart rate, ejection fraction and SV-BA distance response to TCS-DT exposure

As compared to the control group, the 48-hpf larval heart rates were significantly reduced ($p < 0.05$) in the 0.56 and 0.84 mg/L treatments (Fig. S3D). The SV-BA distance is used to mark the looping of the heart tube into the atrium and ventricle, which determines the normal angle between the atria and ventricle (Antkiewicz et al., 2005; Lin et al., 2007), and reflects the change in cardiac looping (Huang et al., 2011). At 120 hpf, TCS-DT exposure caused the SV-BA distance to significantly increase ($p < 0.05$) in a dose-dependent relationship (Fig. S3E). Ejection fraction is often adopted as an indicator of contraction rate, that is, the ratio of the volume of blood drawn from the ventricle in each cardiac cycle to the maximum volume of the entire heart after diastole (Cikes and Solomon, 2016). At 48 hpf, the TCS-DT-exposed ejection fraction showed a significant concentration-dependent decrease compared to the control group (Fig. S3F, $p < 0.05$ or $p < 0.01$). Therefore, we posit that TCS-DT exposure affects cardiac looping and leads to abnormal ventricles, thereby influencing heart function in zebrafish.

3.3. Functional annotation of DEGs and prediction of heart development

To probe the molecular mechanism on phenotypic malformation, we performed deep RNA-seq analysis of the 120-hpf TCS-DT-exposed larvae. Because the expression level of a gene is different in varying tissues and organs of zebrafish, the integrative (synergistic/substrative) expression effect of this gene reflected in RNA-seq of the entire juvenile body will cause omission of some heart development-related DEGs. For this reason, a lowered threshold of differential fold was adopted for screening DEGs, i.e., $|\log_2(\text{fold change})| > 0.5$ and $p < 0.05$. Comparison of TCS-DT treatments to the control group revealed 898 up-regulated and 1134 down-regulated DEGs (Fig. S4A). To clarify the function and location in the metabolic pathway of the DEGs, we annotated DEGs through the GO and KEGG pathways. KEGG pathway analysis showed DEGs mainly distributed in 25 high abundance KEGG pathways, mostly were distributed in three main pathways: metabolism of xenobiotics by cytochrome P450 (ko00980), fatty acid metabolism (ko01212) and drug metabolism-cytochrome P450 (ko00982). Additionally, many DEGs were enriched in adrenergic signaling in cardiomyocytes (Fig. S4B). GO analysis grouped the DEGs into cellular components, biological processes and molecular functions. The cellular components were found to be mainly related to membranes and their integral components, and the biological processes were mainly involved in oxidation-reduction, and happy discovery enriched in cardiac development. Molecular functional analysis indicated activities mainly focused on oxidoreductase activity (Figs. S4C and S5). In addition, the hierarchical cluster analysis of five heart development related GO term's DEGs demonstrated that TCS-DT exposure affected heart development, heart morphogenesis and heart looping (Fig. S5).

3.4. Expression pattern clustering of cardiac development-related genes

Several important genes (17 up-regulation and 22 down-regulation) were retrieved from these GO and KEGG pathways, and they were highly correlated with heart development, heart looping, heart morphogenesis, determination of heart left/right asymmetry, regeneration and adrenergic signaling in cardiomyocytes (Fig. S5 and Fig. 1A). Table S6 lists the detailed information for 39 genes, such as functional description, KEGG pathway, chromosome location, transcript ID, change multiple and *p*-value (DEGs). Among them, 15 genes had identified KEGG pathways while the remaining 24 genes did not (Fig. 1B). To display the underlying mechanism of heart dysgenesis more succinctly, we selected four representative cardiac marker genes (*amhc*, *cmlc2*, *vmhc* and *nkx2.5*) that constitute a network mapping of protein interactions among these DEGs (3 up-regulated and 12 down-regulated genes; Fig. 1C). The pathway interaction network showed the candidate gene interactions split into three branches according to the interaction distance. Seven genes on one branch interacted closely with cardiac markers genes. In contrast, the other two branches had little evidence to support interactive relationships with cardiac marker genes. In the heart, cAMP signaling controls many basic cell functions, such as automatism, contractility and relaxation (Lezoualc'h et al., 2016). Pentose and glucuronate interconversions are related to ventricular development (Singh et al., 2016). For example, the up-regulated *udgh* is mainly distributed in the pathway of pentose and glucuronate metabolism in chromosome 1 for regulation of myocardial oxygen supply, while the up-regulated *sox9b* is located in the cAMP signaling pathway of chromosome 2 (Table S6). Expressions of *mgaa*, *camk2a* and *ppp2r3a* were all down-regulated based on qRT-PCR verification and RNA sequencing (Fig. 1D–E, $p < 0.05$). These results indicate that the DEGs affect cardiac development and differentiation or polarization of maternal cells in the yolk by a complex regulatory network.

3.5. Expression of cardiac marker genes by qRT-PCR and WISH

We evaluated the changes in expression levels and sites of four cardiac marker genes induced by TCS-DT in zebrafish larvae. Compared to the control group, the expression of *amhc* was down-regulated with increasing TCS-DT dose-dependent concentrations. *vmhc* and *cmlc2* were significantly up-regulated at low concentration (0.28 mg/L, $p < 0.05$), while down-regulated at the higher concentrations (0.56 and 0.84 mg/L, $p < 0.05$). In contrast, *nkx*2.5 was significantly down-regulated at 0.28 mg/L ($p < 0.01$), while up-regulated at 0.56 and 0.84 mg/L ($p < 0.05$) (Fig. 1F). This irregular pattern in expression change for *nkx*2.5 may be due to universal expression in the entire juvenile zebrafish body. In addition to the heart, *nkx2.5* was expressed in the notochord, pharyngeal arch and spleen (Searcy et al., 1998; Sehonova et al., 2019). Therefore, the level of *nkx*2.5 mRNA in whole mount larvae did not represent its expression changes exclusively in heart tissue.

To elucidate the distribution and changes of cardiac marker genes, we performed WISH analysis for the four genes in 24, 48 and 72-hpf zebrafish embryos and larvae following exposure to TCS-DT. Expression of the *amhc* gene mainly occurred in the head and heart tissues (Fig. S6A). At 24-hpf, *amhc* gene expression did not show any prominent change (Fig. S6B, $p > 0.05$). At 48 and 72-hpf, the amount of *amhc* expression decreased slowly with increasing TCS-DT concentrations (Figs. S6C–F, $p < 0.05$). For the *nkx2.5* gene, there was no significant difference in the hybrid signal between 24 and 48-hpf, but differences did arise in the 72-hpf embryonic developmental stage. In comparison with the control group, the

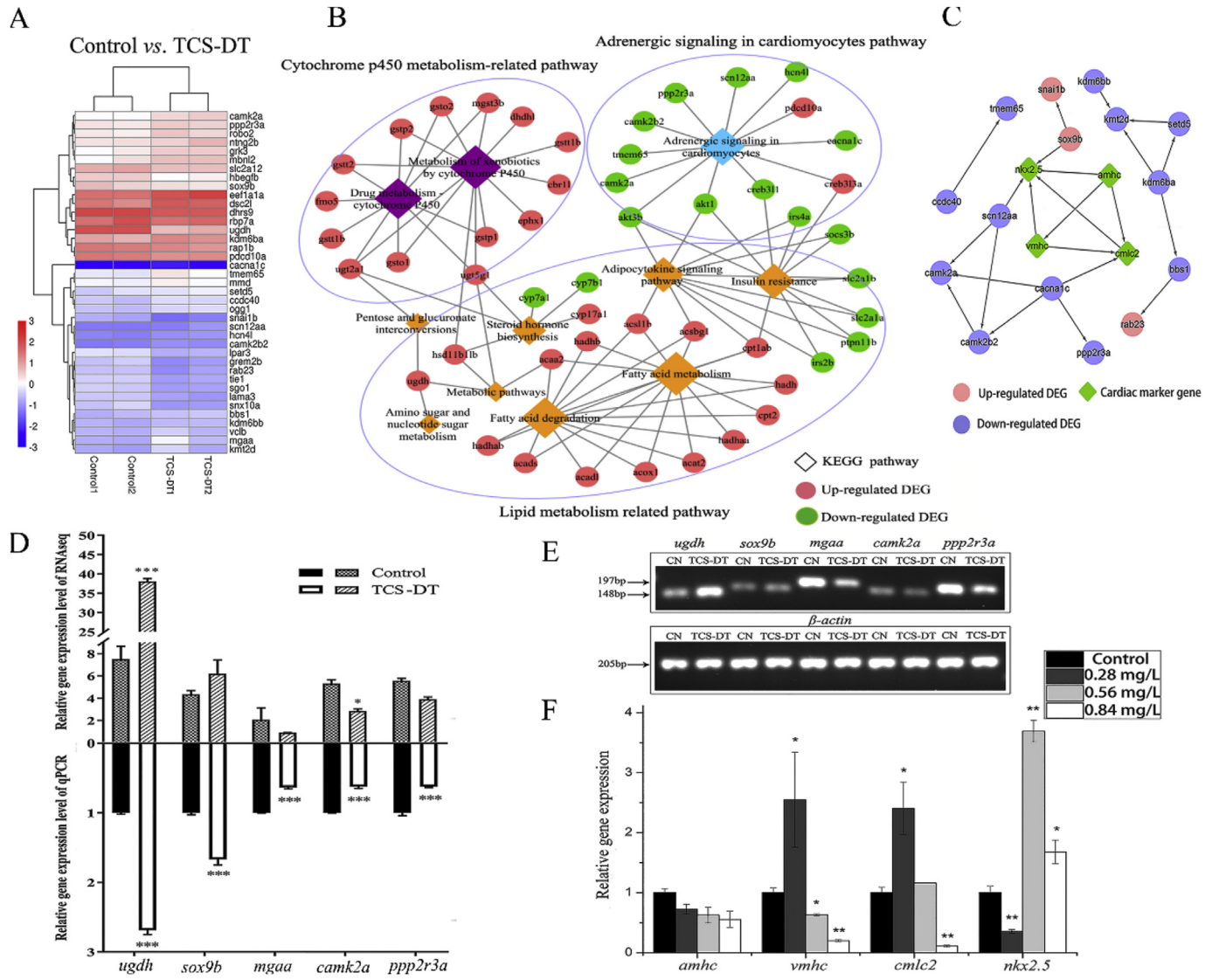

Fig. 1. Screening of cardiac development-related differential expression genes following TCS-DT exposure. Note: (1) A, Heatmap of the 39 DEGs between TCS-DT treatment and control group. Values corresponding to the different colors represent the fold-change (log10 transformed value) of each group. Pink and purple represent up-regulation and down-regulation, respectively; (2) B, KEGG pathway analysis for TCS-DT-exposure group; (3) C, PPI networks of heart-related DEGs. Pink, purple and green nodes indicate the up-regulated, down-regulated and cardiac marker genes, respectively. DEG, differentially expressed genes; PPI, protein-protein network; (4) D-E, Expression of 5 significantly heart-related differential and high-abundance genes among the control and TCS-DT-exposure treatments by qRT-PCR at 120-hpf larvae; (5) F, Expression of cardiac marker genes after exposure to TCS-DT from 6 to 120-hpf; and (6) "*", "**" and "***" indicate significance levels of $p < 0.05$, $p < 0.01$ and $p < 0.001$, respectively. (For interpretation of the references to color in this figure legend, the reader is referred to the Web version of this article.)

expression of *nkx2.5* was significantly decreased in the 0.56 and 0.84 mg/L treatments, but it was not the similar case in the 0.28 mg/L treatment (Fig. S6G, S6G' and S6H, $p < 0.01$).

The *cmlc2* gene showed an obvious down-regulation at 24 and 48-hpf in the 0.56 and 0.84 mg/L treatments relative to the control (Fig. 2A–D, $p < 0.05$). At 72-hpf, the expression level of *cmlc2* was significantly reduced in the 0.84 mg/L treatment group (Fig. 2E–F, $p < 0.001$). Expression of the *vmhc* gene was slightly decreased in response to TCS-DT stress at the 24-hpf stage of early cardiac development, primarily in the heart (Fig. 2G–H, $p < 0.01$). The *vmhc* expression trend continued through the whole embryonic developmental period and remained stable to 72-hpf (Fig. 2I-L, $p < 0.05$). Integration of these results provides compelling evidence that TCS-DT exposure affects atrial and ventricular differentiation.

3.6. Effects of chronic TCS-DT exposure on cardiac development in adult zebrafish

3.6.1. Changes in zebrafish growth and development after chronic TCS-DT exposure

The effects of chronic TCS-DT exposure on zebrafish growth and development were investigated in detail (Fig. 3A–D), such as effects on body length and width. Body mass index (BMI) is often used as a measure of obesity (Okorodudu et al., 2010). There was no significant difference in cardiac morphology (Fig. 3E–H) and adult body length (Fig. 3Q). Compared to the control group, the BMI and body width of 90-dpf zebrafish in the TCS-DT treatments significantly increased ($p < 0.05$; Fig. 3Q and S7A). In terms of sexual differentiation, the chronic TCS-DT exposure to zebrafish resulted in increasing female percentage (>58%), demonstrating their

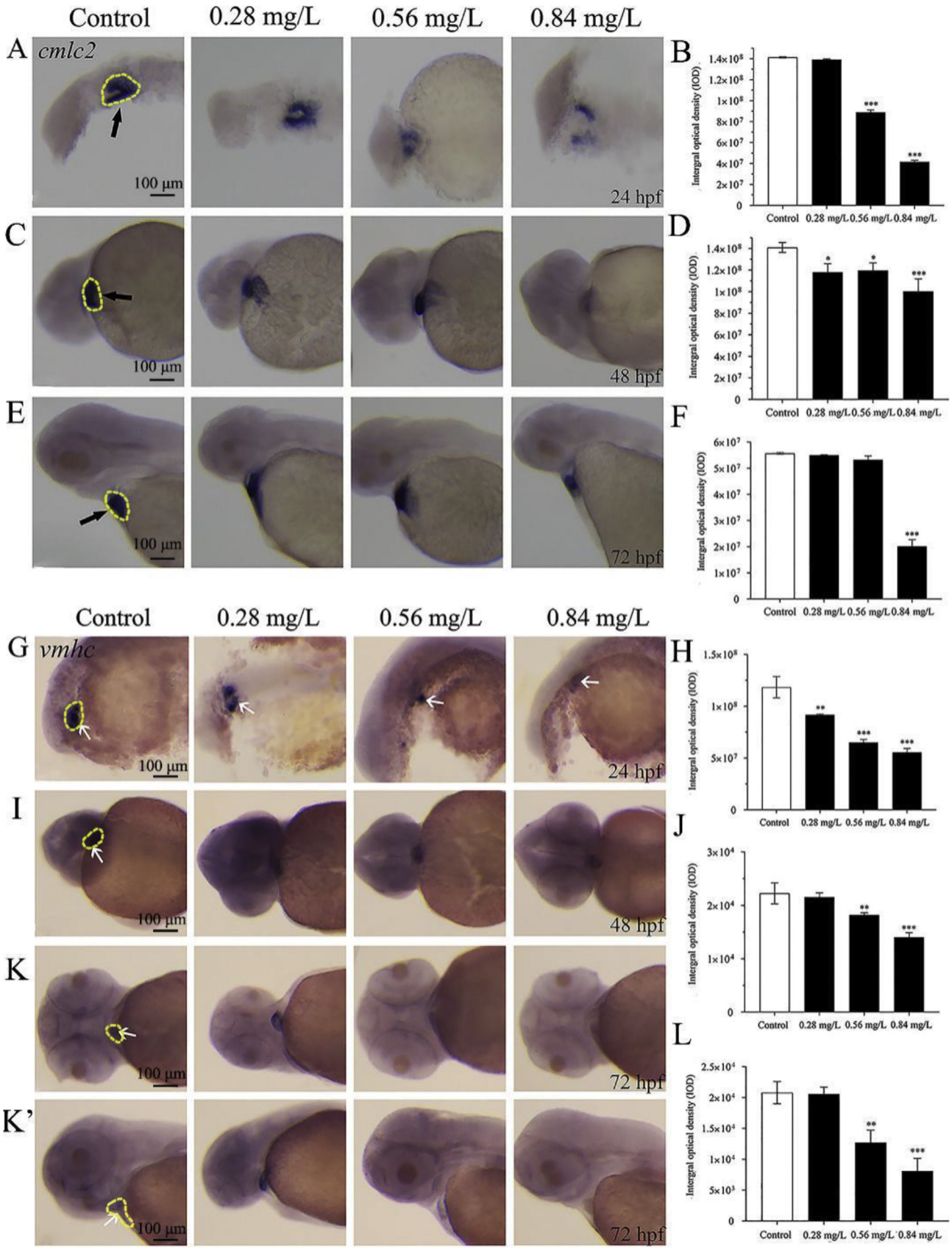

Fig. 2. Differential expression of two cardiac marker genes (cmlc2 and vmhc) by WISH. Note: (1) A, C and E, WISH of cmlc2 expression in 24, 48 and 72-hpf larvae, respectively; (2) B, D and F, IODs of cmlc2 expression in 24, 48 and 72-hpf zebrafish larvae, respectively; (3) G, I, K and K′, WISH of vmhc expression in 24, 48 and 72-hpf larvae, respectively; (4) H, J and L, IODs of vmhc expression in 24, 48 and 72-hpf zebrafish larvae, respectively; (5) Arrows indicate the heart; (6) Scale bars: 100 μm; and (7) "*", "**" and "***" indicate significance levels of $p < 0.05$, $p < 0.01$ and $p < 0.001$, respectively.

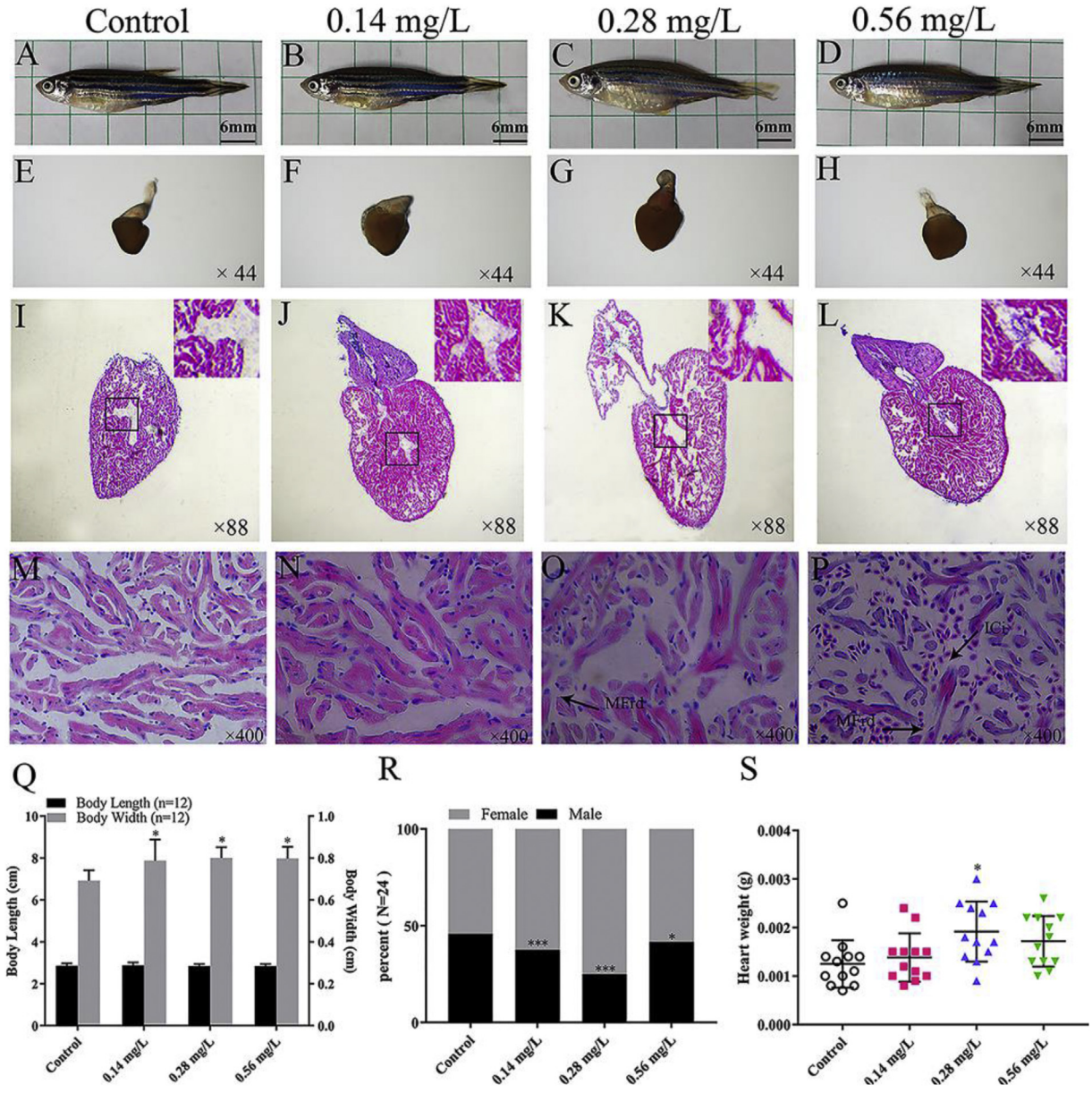

Fig. 3. Growth index and histopathological observation of zebrafish heart after chronic TCS-DT exposure. Note:(1) A-D, morphology of 90-dpf zebrafish after chronic TCS-DT exposure; (2) E-F, morphology of 90-dpf heart tissue after chronic TCS-DT exposure; (3) I-L, longitudinal section images of the whole heart; Inset figure shows the enlarged portion of black box area; (4) M-P, H&E staining of adult heart tissues; (5) Q, body length and body width; R, ratio of female to male zebrafish; S, heart weight; (6) MFrd, rupture and dissolution of myocardial fibers; ICi, inflammatory cell infiltration; and (7) "*", "**" and "***" indicate significance levels of $p < 0.05$, $p < 0.01$ and $p < 0.001$, respectively.

prominent estrogen disrupting effects (Fig. 3R). Meanwhile, both cardiac organ index and heart weight showed slightly increasing trends with increasing TCS-DT concentrations when compared to the control group (Figs. 3S and S7B).

Compared to the control group, CK-MB activity and triglyceride (TG) levels in adult heart were significantly higher in the TCS-DT treatments ($p < 0.05$; Figs. S7C–D). SOD levels were significantly increased in the 0.14 and 0.28 mg/L treatments, but decreased in the 0.56 mg/L treatment ($p < 0.001$; Fig. S7E). Notably, LDH levels were increased in the 0.14 mg/L treatment ($p < 0.05$), but decreased significantly in the 0.28 and 0.56 mg/L treatments ($p < 0.001$; Fig. S7F). Changes in these enzymatic activities indicate damage to cardiomyocytes (Zhou et al., 2008), suggesting the presence of myocarditis. In general, these findings demonstrate that chronic TCS-DT exposure affects the normal growth and development of zebrafish, especially with respect to triggering heart diseases.

3.6.2. TCS-DT induced myocardial ablation and mitochondrial damage

In this study, three TCS-DT concentrations (0.14, 0.28, and 0.56 mg/L) were selected as sublethal doses to assess chronic toxicity effect. Following continuous TCS-DT exposure from 30 to 90-dpf, zebrafish heart tissues were dissected and H&E-stained (Fig. 3I-P). In the control group, myocardial cells were intact (Fig. 3M), the nucleus was ellipsoidal and neatly arranged, and myofilament fiber was continuous. However, some myofilaments were damaged in the 0.14 mg/L treatment, and severely myofibrillar fiber rupture and inflammatory cell infiltration were observed in the 0.28 and 0.56 mg/L treatments (Fig. 3N–P). Masson's trichrome staining showed cardiomyocytes with well-preserved cytoplasm and prominent nuclei in the control group. In contrast, TCS-DT exposure led to varying degrees of myofilament rupture with a prominent dose-dependence. For example, the

compacted nuclei in the 0.56 mg/L treatment indicated inflammatory infiltration, and a small amount of collagen fibers, suggesting possible cardiac fibrosis (Fig. 4A).

We examined ultrastructural sections of zebrafish heart tissue by TEM to assess the effects of long-term TCS-DT exposure on subcellular structure injury to cardiomyocytes. The control group had a nucleus that was clear and complete, the matrix electron density was uniform. Complete discs were clearly visible in myocardial fibers, the intercellular filaments were connected tightly (Fig. 4B), and myocardial fibers were arranged in a continuous and regular manner. Further, the Z line, the H band and the light and dark bands were clearly distinguishable (Fig. 4C). Additionally, the electron density of mitochondria was clear, the crest neatly arranged and the double-layer membrane clearly visible (Fig. 4D). In the 0.14 mg/L treatment group, the nuclear membrane was slightly wrinkled, the number of intercalated disks decreased, the gap between the filaments was some evidence of edema (Fig. 4B). Further, the H band and the light and dark bands were difficult to distinguish, and there was myofilament breakage (Fig. 4C). Additionally, there was structural dissolution in mitochondria (Fig. 4D). As the TCS-DT concentration increased to 0.28 and 0.56 mg/L, and even the discs were indistinguishable, the myocardial cells showed signs of edema (Fig. 4B). The Z line was also difficult to distinguish (Fig. 4C). These results indicate that exposure to increasing concentrations of TCS-DT causes serious damage to the myocardial subcellular structure that can lead to myocardial inflammation and heart failure.

4. Discussion

The first organ to form and function in vertebrate embryos is the heart (Yin and Pacifici, 2001), which develops from endocardial progenitors and cardiomyocytes (Bakkers, 2011). The *nkx2.5* gene is often regarded as a cardiac progenitor cell marker, ensuring the qualitative or quantitative characteristics of the ventricles during the initial differentiation of cardiac muscle cells (Targoff et al., 2013). In this study, we demonstrated that the expression of *nkx2.5* was significantly reduced after exposure to TCS-DT. The

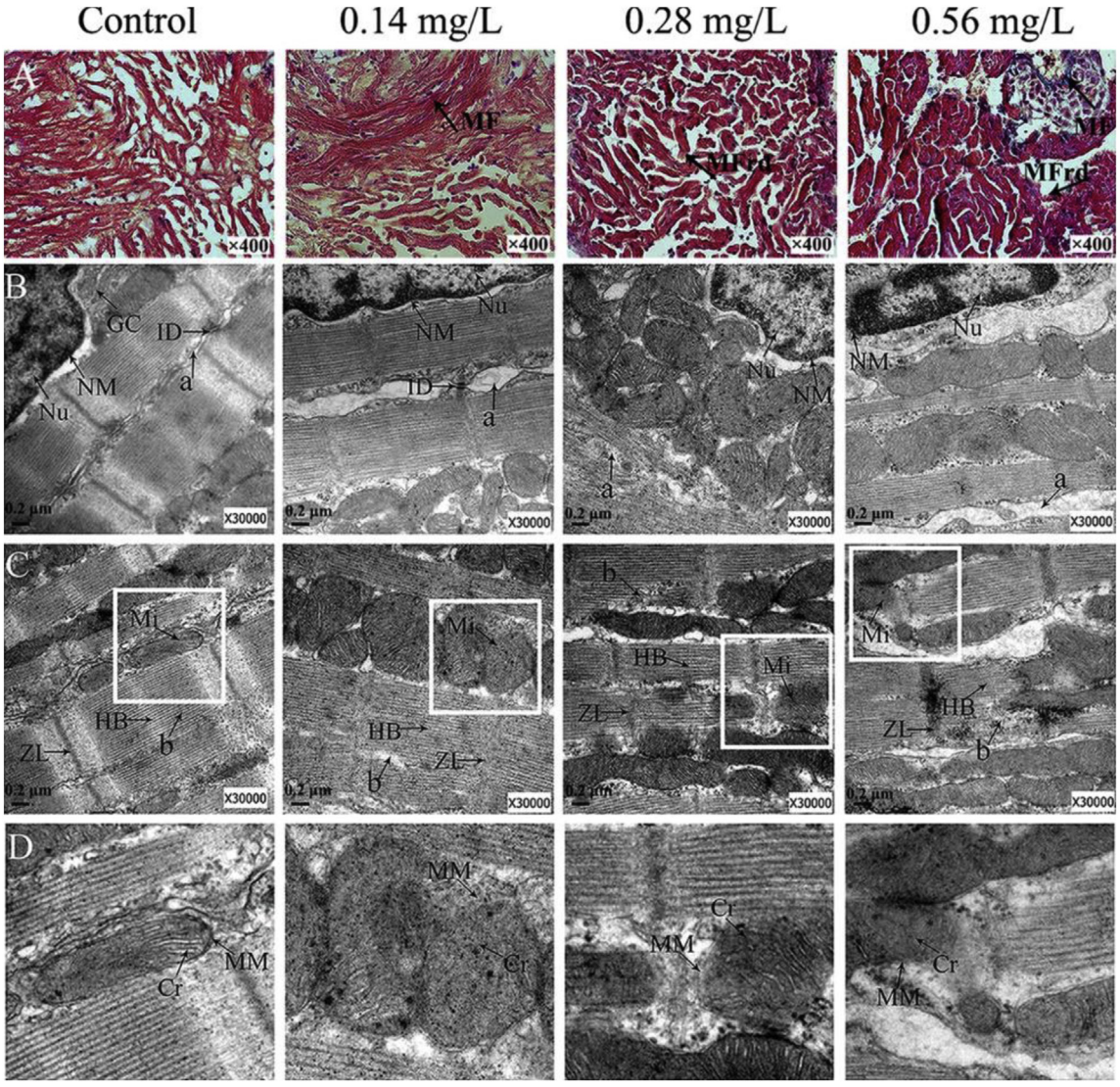

Fig. 4. Masson's trichrome staining and TEM images of adult heart tissues. Note:(1) A, Masson's trichrome staining of 90-dpf zebrafish heart; (2) B-D, TEM images of cardiomyocytes in zebrafish; (3) MF, myocardial fibrosis; ICi, inflammatory cell infiltration; Nu nucleus; GC, Golgi complex; NM, Nuclear membrane; ID, Intercalated disc; Mi, Mitochondrion; ZL, Z line; HB, H-band; MM, mitochondrial membrane; Cr, crista; (4) "a" arrow indicates myocutaneous space; "b" arrow indicates muscle rupture and dissolution; (5) Fig. 4D shows the magnified part of white box in Fig. 4C.

change in the expression level of *nkx2.5* led to an imbalance of cardiac progenitor cell differentiation, further initiating abnormal myocardial growth and destruction of ventricular morphology. Zebrafish heart is composed of a single atrium and ventricle separated by atrial valves (Sarmah and Marrs, 2016). The *vmhc* is a ventricular myosin heavy chain gene that plays an important role in heart construction (Zhang and Xu, 2009; Shih et al., 2015). Further, *cmlc2* is used as a fluorescent cardiac marker in the construction of transgenic zebrafish (Chen et al., 2008). Additionally, *amhc* is related to the contraction of the atrial myofibrils that participate in heart contraction and construction of the cardiac muscle skeleton (Berdougo et al., 2003; Abu-Daya et al., 2009). Both atria and ventricles were damaged by TCS-DT exposure, suggesting the jointly toxic effects of TCS and its derivatives.

Based on the qRT-PCR and RNA-seq results, we constructed a regulatory network to illustrate the adverse effects of TCS-DT on heart development (Fig. 5). In brief, TCS-DT induced cardiotoxicity resulted from disruption of several signaling pathways: (i) cAMP signaling pathway, (ii) adrenergic signaling in cardiomyocytes, and (iii) pentose and glucuronate interconversions. Moreover, when traced back to the regulatory mechanism, the transcription levels of cardiac development-related genes, including *ugdh*, *sox9b*, *ppp2r3a* and *camk2a*, were dysregulated following exposure to TCS-DT. These genes play critical roles in lipid balance and cardiac morphogenesis. For example, *ugdh* functions in cardiac valve formation (Walsh and Stainier, 2001), and *sox9b* in cardiomyocytes for cardiac morphogenesis (Gawdzik et al., 2018). *mgaa* as a MAX dimerization protein, is crucial for heart organ development (Rikin and Evans, 2010). This study demonstrated that *sox9b* was closely related to the formation of pericardial walls, and the formation and

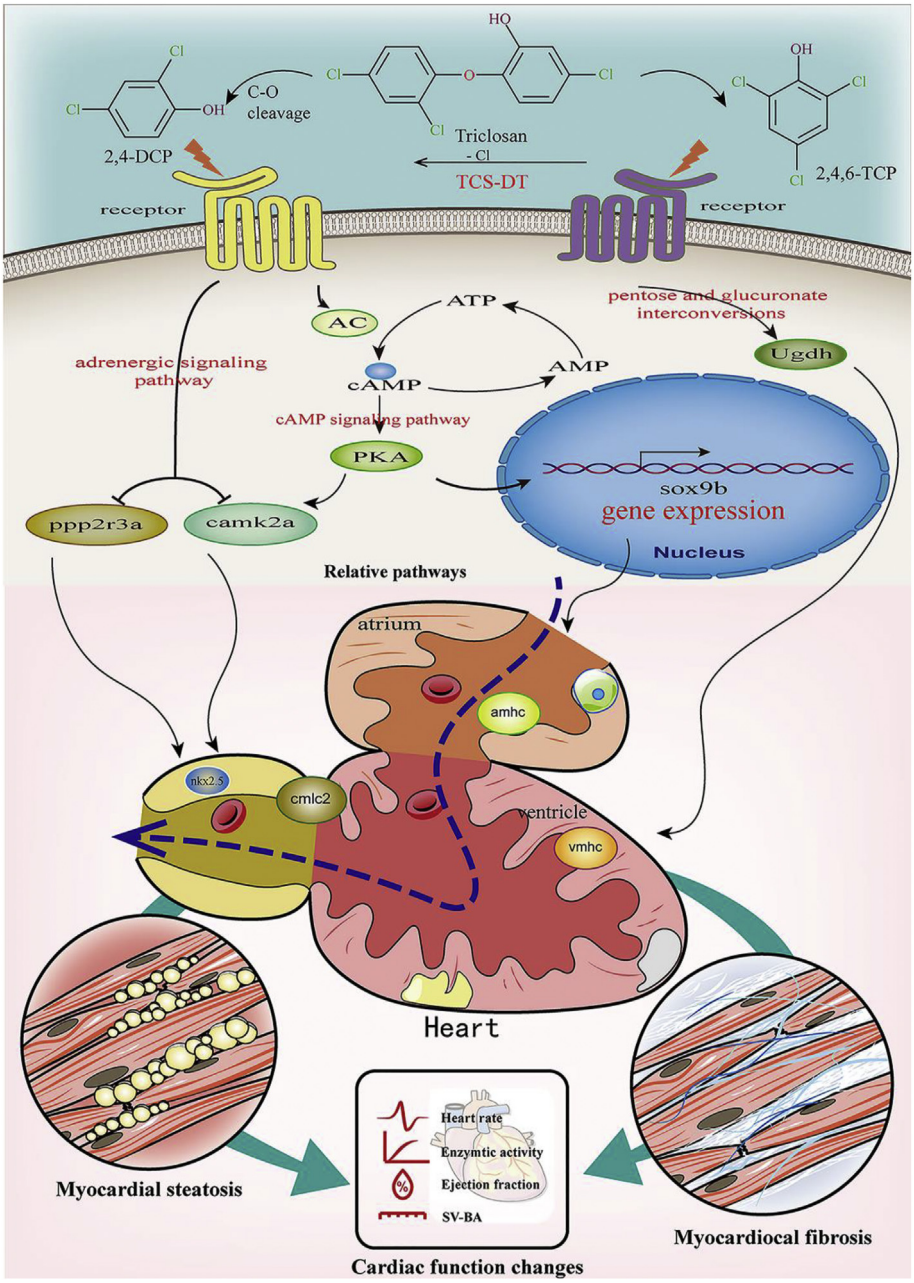

Fig. 5. Predictive regulatory mechanism for TCS-DT exposure on zebrafish cardiotoxicity.

migration of epicardial layers around the heart. After exposure to TCDD, the expression of *sox9b* was decreased, which prevented the formation of heart (Hofsteen et al., 2013). However, our experimental results showed the transcription level of *sox9b* was up-regulated by TCS-DT exposure, highlighting the need for further molecular-level research to resolve expression trends of *sox9b* upon exposure to environmental pollutants. Although a certain number of DEGs related to heart development were identified, their detected rate was relatively low due to only two biological replicates for RNA-seq. Under the same RNA-seq depth, the increase of biological replicate number is in concomitant with increase in the detection rate of DEGs (Khang and Lau, 2015). In further research, we will adopt three or more biological replicates for RNA-seq samples in each control or treatment group. It is worth noting that because the larval heart is very difficult to collect, single-cell sequencing technology can be used to evaluate the toxic effect of TCS-DT exposure on larval heart development (Weinberger et al., 2020).

Recent studies revealed that adrenergic signaling enhanced overall cardiac myocyte cohesion. Adrenaline stimulated the heart muscle and contributed to the heart function adapt to sympathetic nerve activity (Schinner et al., 2017). TCS-DT exposure may have a prominent effect on adrenergic signaling in the cardiomyocytes. The circadian system can predict participation in time-related behaviors (Antle and Silver, 2016). These presumptions are consistent with the results of our diurnal behavioral experiments, and changes in sympathetic nerve activity might further affect behavioral abnormalities. Early-state metabolic syndrome may enhance β-adrenergic stimulation and trigger production of mitochondrial reactive oxygen species (ROS) in cardiomyocytes. Increased ROS production may result in severe pathological changes and contribute to cardiac dysfunction (Llano-Diez et al., 2016). Importantly, changes in SOD activity control the level of ROS (Wang et al., 2018). SOD is the first line of antioxidant defense system. Under the low concentration of TCS-DT exposure, the SOD activity of heart tissue increases, strengthening the elimination of active oxygen free radicals, so as to avoid the oxidative damage to organism tissues (Li et al., 2012), but they will trigger oxidative stress in the absence of downstream enzymes sufficient to detoxify the final SOD product (Poznyak et al., 2020). Decreased SOD levels are an important indicator of oxidative stress (Akila and Vennila, 2016). Under high concentration of TCS-DT exposure, SOD activity decreased, indicating that oxidative damage occurred in the heart of adult zebrafish. Beyond that, the GO and KEGG pathways mainly involved lipid metabolism processes, which contributed to the occurrence of yolk cysts. TG could supply efficient energy for the heart; however, too much TG might produce excess lipid accumulation, contributing to heart failure (Goldberg, 2018), which implied that cardiomyocyte steatosis might result from chronic TCS-DT stress.

5. Conclusion

Herein, we evaluated the cardiac developmental toxicity of TCS-DT to zebrafish larvae and found that it caused a series of cardiac malformations: pericardial edema, heart bleeding and hypertrophy as well as myocardial fibrosis. Based on these phenotype abnormalities, TCS-DT induced cardiotoxic molecular mechanism was investigated in detail. Cardiac development marker genes (*vhmc*, *nkx2.5*, *amhc* and *cmlc2*) and adrenergic signaling in cardiomyocytes showed the down-regulated trends upon exposure to TCS-DT. Besides, chronic TCS-DT exposure resulted in prominently abnormal changes in a series of cardiac functions-related biomarkers (TG, LDH, CK-MB and SOD), consequently providing strong evidence for cardiac pathological responses. Due to the coexistence of TCS and its derivatives in real-world aquatic environment, these data are conductive to reveal the molecular mechanism of cardiac toxicity under the joint exposure to TCS, 2,4-DCP and 2,4,6-TCP, also providing a more comprehensive risk assessment.

Declaration of competing interest

The author reports no conflicts of interest in this work.

CRediT authorship contribution statement

Danting Wang: Writing - original draft, Writing - review & editing, Methodology, Formal analysis, Data curation, Conceptualization. **Yuhuan Zhang:** Conceptualization, Methodology, Investigation, Formal analysis, Data curation. **Jieyi Li:** Data curation, Methodology. **Randy A. Dahlgren:** Writing - review & editing. **Xuedong Wang:** Methodology, Investigation, Writing - review & editing. **Haishan Huang:** Supervision, Project administration. **Huili Wang:** Conceptualization, Supervision, Project administration, Funding acquisition.

Acknowledgement

This work was jointly supported by the National Natural Science Foundation of China (31770552), and Natural Science Foundation of Jiangsu Province (BK20191455).

Appendix A. Supplementary data

Supplementary data to this article can be found online at https://doi.org/10.1016/j.envpol.2020.114995.

References

Abu-Daya, A., Sater, A.K., Wells, D.E., Mohun, T.J., Zimmerman, L.B., 2009. Absence of heartbeat in the Xenopus tropicalis mutation muzak is caused by a nonsense mutation in cardiac myosin myh6. Dev. Biol. 336, 20–29.
Adgent, M.A., Rogan, W.J., 2015. Triclosan and prescription antibiotic exposures and enterolactone production in adults. Environ. Res. 142, 66–71.
Akila, P., Vennila, L., 2016. Chlorogenic acid a dietary polyphenol attenuates isoproterenol induced myocardial oxidative stress in rat myocardium: an in vivo study. Biomed. Pharmacother. 84, 208–214.
Antkiewicz, D.S., Burns, C.G., Carney, S.A., Peterson, R.E., Heideman, W., 2005. Heart malformation is an early response to TCDD in embryonic zebrafish. Toxicol. Sci. 84, 368–377.
Antle, M.C., Silver, R., 2016. Circadian insights into motivated behavior. Curr. Top Behav. Neurosci. 27, 137–169.
Bakkers, J., 2011. Zebrafish as a model to study cardiac development and human cardiac disease. Cardiovasc. Res. 91, 279–288.
Bedoux, G., Roig, B., Thomas, O., Dupont, V., Le Bot, B., 2011. Occurrence and toxicity of antimicrobial triclosan and by-products in the environment. Environ. Sci. Pollut. Res. 19, 1044–1065.
Berdougo, E., Coleman, H., Lee, D.H., Stainier, D.Y., Yelon, D., 2003. Mutation of weak atrium/atrial myosin heavy chain disrupts atrial function and influences ventricular morphogenesis in zebrafish. Development 130, 6121–6129.
Cao, X., Hua, X., Wang, X., Chen, L., 2017. Exposure of pregnant mice to triclosan impairs placental development and nutrient transport. Sci. Rep. UK 7, 44803.
Chen, Z., Huang, W., Dahme, T., Rottbauer, W., Ackerman, M.J., Xu, X., 2008. Depletion of zebrafish essential and regulatory myosin light chains reduces cardiac function through distinct mechanisms. Cardiovasc. Res. 79, 97–108.
Chen, Z., Wang, Z., 2012. Functional study of hyperpolarization activated channel (I_h) in *Drosophila* behavior. Sci. China Life Sci. 55, 2–7.
Cikes, M., Solomon, S.D., 2016. Beyond ejection fraction: an integrative approach for assessment of cardiac structure and function in heart failure. Eur. Heart J. 37, 1642–1650.
Dann, A.B., Hontela, A., 2011. Triclosan: environmental exposure, toxicity and mechanisms of action. J. Appl. Toxicol. 31, 285–311.
Du, P., Zhao, H., Li, H., Zhang, D., Huang, C.H., Deng, M., Liu, C., Cao, H., 2016. Transformation, products, and pathways of chlorophenols via electro-enzymatic catalysis: how to control toxic intermediate products. Chemosphere 144, 1674–1681.
Einhorn, Z., Trapani, J.G., Liu, Q., Nicolson, T., 2012. Rabconnectin3α promotes stable activity of the H+ pump on synaptic vesicles in hair cells. J. Neurosci. 32, 11144–11156.

Feng, Y., Zhang, P., Zhang, Z., Shi, J., Jiao, Z., Shao, B., 2016. Endocrine disrupting effects of triclosan on the placenta in pregnant rats. PloS One 11, e0154758.
Gao, J., Liu, L., Liu, X., Zhou, H., Huang, S., Wang, Z., 2008. Levels and spatial distribution of chlorophenols-2,4-Dichlorophenol, 2,4,6-trichlorophenol, and pentachlorophenol in surface water of China. Chemosphere 71, 1181–1187.
Gawdzik, J.C., Yue, M.S., Martin, N.R., Elemans, L.M., Lanham, K.A., Heideman, W., Rezendes, R., Baker, T.R., Taylor, M.R., Plavicki, J.S., 2018. Sox9b is required in cardiomyocytes for cardiac morphogenesis and function. Sci. Rep. 8, 1–16.
Goldberg, I.J., 2018. 2017 George Lyman Duff Memorial Lecture: fat in the blood, fat in the artery, fat in the heart: triglyceride in physiology and disease. Arterioscl Throm Vas 38, 700–706.
Ho, J.C., Hsiao, C., Kawakami, K., William, K., 2016. Triclosan (TCS) exposure impairs lipid metabolism in zebrafish embryos. Aquat. Toxicol. 173, 29–35.
Hofsteen, P., Plavicki, J., Johnson, S.D., Peterson, R.E., Heideman, W., 2013. Sox9b is required for epicardium formation and plays a role in TCDD-induced heart malformation in zebrafish. Mol. Pharmacol. 84, 353–360.
Huang, D.W., Sherman, B.T., Lempicki, R.A., 2008. Bioinformatics enrichment tools: paths toward the comprehensive functional analysis of large gene lists. Nucleic Acids Res. 37, 1–13.
Huang, Q., Fang, C., Wu, X., Fan, J., Dong, S., 2011. Perfluorooctane sulfonate impairs the cardiac development of a marine medaka (*Oryzias melastigma*). Aquat. Toxicol. 105, 71–77.
Jiang, Z., Yang, T., Zhang, Y., Wang, J., 2015. Characterization and evaluation of the efficiency of SiO_2/tetra-α-(2,4-di-tert-butylphenoxy)-phthalocyaninato zinc nanocomposite as photosensitizers for oxidation of 2,4,6-trichlorophenol. Environ. Technol. 36, 1643–1650.
Jin, X., Gao, J., Zha, J., Xu, Y., Wang, Z., Richardson, K.L., 2012. A tiered ecological risk assessment of three chlorophenols in Chinese surface waters. Environ. Sci. Pollut. R 19, 1544–1554.
Kanehisa, M., Araki, M., Goto, S., Hattori, M., Hirakawa, M., Itoh, M., Katayama, T., Kawashima, S., Okuda, S., Tokimatsu, T., 2007. KEGG for linking genomes to life and the environment. Nucleic Acids Res. 36, D480–D484.
Khang, T.F., Lau, C.Y., 2015. Getting the most out of RNA-seq data analysis. PeerJ 3, e1360.
Kim, J., Oh, H., Ryu, B., Kim, U., Lee, J.M., Jung, C.R., 2018. Triclosan affects axon formation in the neural development stages of zebrafish embryos (*Danio rerio*). Environ. Pollut. 236, 304–312.
Lenz, K.A., Pattison, C., Ma, H., 2017. Triclosan (TCS) and triclocarban (TCC) induce systemic toxic effects in a model organism the nematode Caenorhabditis elegans. Environ. Pollut. 231, 462–470.
Lezoualc'h, F., Fazal, L., Laudette, M., Conte, C., 2016. Cyclic AMP sensor EPAC proteins and their role in cardiovascular function and disease. Circ. Res. 118, 881–897.
Li, E., Bolser, D.G., Kroll, K.J., Brockmeier, E.K., Francesco, F., Denslow, N.D., 2018. Comparative toxicity of three phenolic compounds on the embryo of fathead minnow, Pimephales promelas. Aquat. Toxicol. 201, 66–72.
Li, H., Xie, Y.H., Yang, Q., Wang, S.W., Zhang, B.L., Wang, J.B., Cao, W., Bi, L.L., Sun, J.Y., Miao, S., 2012. Cardioprotective effect of paeonol and danshensu combination on isoproterenol-induced myocardial injury in rats. PloS One 7, e48872.
Li, J., Liu, J., Zhang, Y., Wang, X., Li, W., Zhang, H., Wang, H., 2016. Screening on the differentially expressed miRNAs in zebrafish (*Danio rerio*) exposed to trace β-diketone antibiotics and their related functions. Aquat. Toxicol. 178, 27–38.
Li, Y.F., Canário, A.V., Power, D.M., Campinho, M.A., 2019. Ioxynil and diethylstilbestrol disrupt vascular and heart development in zebrafish. Environ. Int. 124, 511–520.
Liao, Y., Smyth, G.K., Shi, W., 2014. FeatureCounts: an efficient general purpose program for assigning sequence reads to genomic features. Bioinformatics 30, 923–930.
Lin, C.C., Hui, M.N., Cheng, S.H., 2007. Toxicity and cardiac effects of carbaryl in early developing zebrafish (*Danio rerio*) embryos. Toxicol. Appl. Pharmacol. 222, 159–168.
Lin, J., Wang, C., Liu, J., Dahlgren, R.A., Ai, W., Zeng, A., Wang, X., Wang, H., 2017. Upstream mechanisms for up-regulation of miR-125b from triclosan exposure to zebrafish (*Danio rerio*). Aquat. Toxicol. 193, 256–267.
Liu, J., Sun, L., Zhang, H., Shi, M., Dahlgren, R.A., Wang, X., Wang, H., 2018. Response mechanisms to joint exposure of triclosan and its chlorinated derivatives on zebrafish (*Danio rerio*) behavior. Chemosphere 193, 820–832.
Llano-Diez, M., Sinclair, J., Yamada, T., Zong, M., Fauconnier, J., Zhang, S.J., Katz, A., Jardemark, K., Westerblad, H., Andersson, D.C., Lanner, J.T., 2016. The role of reactive oxygen species in β-adrenergic signaling in cardiomyocytes from mice with the metabolic syndrome. PloS One 11, e0167090.
Lu, S., Wang, N., Ma, S., Hu, X., Kang, L., Yu, Y., 2019. Parabens and triclosan in shellfish from Shenzhen coastal waters: bioindication of pollution and human health risks. Environ. Pollut. 246, 257–263.
Lubrano, V., Balzan, S., 2015. Enzymatic antioxidant system in vascular inflammation and coronary artery disease. World J. Exp. Med. 5, 218–224.
Matrone, G., Maqsood, S., Taylor, J., Mullins, J.J., Tucker, C.S., Denvir, M.A., 2014. Targeted laser ablation of the zebrafish larval heart induces models of heart block, valvular regurgitation, and outflow tract obstruction. Zebrafish 11, 536–541.
McCurley, A.T., Callard, G.V., 2008. Characterization of housekeeping genes in zebrafish: male-female differences and effects of tissue type, developmental stage and chemical treatment. BMC Mol. Biol. 9, 102.
Meador, J.P., Yeh, A., Gallagher, E.P., 2018. Adverse metabolic effects in fish exposed to contaminants of emerging concern in the field and laboratory. Environ. Pollut. 236, 850–861.
Morales, S., Canosa, P., Rodríguez, I., Rubí, E., Cela, R., 2005. Microwave assisted extraction followed by gas chromatography with tandem mass spectrometry for the determination of triclosan and two related chlorophenols in sludge and sediments. J. Chromatogr. A 1082, 128–135.
Mortazavi, A., Williams, B.A., McCue, K., Schaeffer, L., Wold, B., 2008. Mapping and quantifying mammalian transcriptomes by RNA-Seq. Nat. Methods 5, 621–628.
Okorodudu, D.O., Jumean, M.F., Montori, V.M., Romero-Corral, A., Somers, V.K., Erwin, P.J., Lopez-Jimenez, F., 2010. Diagnostic performance of body mass index to identify obesity as defined by body adiposity: a systematic review and meta-analysis. Int. J. Obes. 34, 791–799.
Olaniyan, L.W.B., Mkwetshana, N., Okoh, A.I., 2016. Triclosan in water, implications for human and environmental health. SpringerPlus 5, 1639–1655.
Parastar, S., Ebrahimpour, K., Hashemi, M., Maracy, M.R., Kelishadi, R., 2018. Association of urinary concentrations of four chlorophenol pesticides with cardiometabolic risk factors and obesity in children and adolescents. Environ. Sci. Pollut. R 25, 4516–4523.
Poss, K.D., Wilson, L.G., Keating, M.T., 2002. Heart regeneration in zebrafish. Science 298, 2188–2190.
Poznyak, A.V., Grechko, A.V., Orekhova, V.A., Chegodaev, Y.S., Wu, W.K., Orekhov, A.N., 2020. Oxidative stress and antioxidants in atherosclerosis development and treatment. Biology 9, 60.
Rikin, A., Evans, T., 2010. The tbx/bHLH transcription factor mga regulates gata4 and organogenesis. Dev. Dynam. 239, 535–547.
Ruszkiewicz, J.A., Li, S., Rodriguez, M.B., Aschner, M., 2017. Is triclosan a neurotoxic agent? J. Toxicol. Environ. Health B 20, 104–117.
Saley, A., Hess, M., Miller, K., Howard, D., King-Heiden, T.C., 2016. Cardiac toxicity of triclosan in developing zebrafish. Zebrafish 13, 399–404.
Sarmah, S., Marrs, J., 2016. Zebrafish as a vertebrate model system to evaluate effects of environmental toxicants on cardiac development and function. Int. J. Mol. Sci. 17, 2123–2138.
Schinner, C., Vielmuth, F., Rötzer, V., Hiermaier, M., Radeva, M.Y., Co, T.K., Hartlieb, E., Schmidt, A., Imhof, A., Messoudi, A., Horn, A., Schlipp, A., Spindler, V., Waschke, J., 2017. Adrenergic signaling strengthens cardiac myocyte cohesion. Circ. Res. 120, 1305–1317.
Searcy, R.D., Vincent, E.B., Liberatore, C.M., Yutzey, K.E., 1998. A gata-dependent nkx2-5 regulatory element activates early cardiac gene expression in transgenic mice. Development 125, 4461–4470.
Sehonova, P., Hodkovicova, N., Urbanova, M., Örn, S., Blahova, J., Svobodova, Z., Faldyna, M., Chloupek, P., Briedikova, K., Carlsson, G., 2019. Effects of antidepressants with different modes of action on early life stages of fish and amphibians. Environ. Pollut. 254, 112999.
Shih, Y.H., Zhang, Y., Ding, Y., Ross, C.A., Li, H., Olson, T.M., Xu, X., 2015. Cardiac transcriptome and dilated cardiomyopathy genes in zebrafish. Circ-Cardiovasc Gene. 8, 261–269.
Singh, A.R., Sivadas, A., Sabharwal, A., Vellarikal, S.K., Jayarajan, R., Verma, A., Kapoor, S., Joshi, A., Scaria, V., Sivasubbu, S., 2016. Chamber specific gene expression landscape of the zebrafish heart. PloS One 11, e0147823.
Targoff, K.L., Colombo, S., George, V., Schell, T., Kim, S.H., Solnicakrezel, L., Yelon, D., 2013. Nkx genes are essential for maintenance of ventricular identity. Development 140, 4203–4213.
Tixier, C., Singer, H.P., Canonica, S., Müller, S.R., 2002. Phototransformation of triclosan in surface waters: a relevant elimination process for this widely used biocide Laboratory studies, field measurements, and modeling. Environ. Sci. Technol. 36, 3482–3489.
Thisse, C., Thisse, B., 2008. High-resolution in situ hybridization to whole-mount zebrafish embryos. Nat. Protoc. 3, 59–69.
Thomaidi, V.S., Matsoukas, C., Stasinakis, A.S., 2017. Risk assessment of triclosan released from sewage treatment plants in European rivers using a combination of risk quotient methodology and Monte Carlo simulation. Sci. Total Environ. 603–604, 487–494.
Trapnell, C., Williams, B.A., Pertea, G., Mortazavi, A., Kwan, G., Van Baren, M.J., Salzberg, S.L., Wold, B.J., Pachter, L., 2010. Transcript assembly and quantification by RNA-Seq reveals unannotated transcripts and isoform switching during cell differentiation. Nat. Biotechnol. 28, 511–515.
Walsh, E.C., Stainier, D.Y., 2001. UDP-glucose dehydrogenase required for cardiac valve formation in zebrafish. Science 293, 1670–1673.
Wang, C.F., Tian, Y., 2015. Reproductive endocrine-disrupting effects of triclosan: population exposure, present evidence and potential mechanisms. Environ. Pollut. 206, 195–201.
Wang, L., Wang, S., Li, W., 2012. RSeQC: quality control of RNA-seq experiments. Bioinformatics 28, 2184–2185.
Wang, Y., Branicky, R., Noë, A., Hekimi, S., 2018. Superoxide dismutases: dual roles in controlling ROS damage and regulating ROS signaling. J. Cell Biol. 217, 1915–1928.
Weinberger, M., Simões, F.C., Patient, R., Sauka-Spengler, T., Riley, P.R., 2020. Functional heterogeneity within the developing zebrafish epicardium. Dev. Cell 52, 574–590 e6.
Xia, X., Hua, C., Xue, S., Shi, B., Gui, G., Zhang, D., Wang, X., Guo, L., 2016. Response of selenium-dependent glutathione peroxidase in the freshwater bivalve Anodonta woodiana exposed to 2,4-dichlorophenol, 2,4,6-trichlorophenol and pentachlorophenol. Fish Shellfish Immunol. 55, 499–509.
Yin, M., Pacifici, M., 2001. Vascular regression is required for mesenchymal condensation and chondrogenesis in the developing limb. Dev. Dynam. 222, 522–533.

Young, M.D., Wakefield, M.J., Smyth, G.K., Oshlack, A., 2010. Gene ontology analysis for RNA-seq: accounting for selection bias. Genome Biol. 11, R14.
Yueh, M.F., Tukey, R.H., 2016. Triclosan: a widespread environmental toxicant with many biological effects. Annu. Rev. Pharmacol. 56, 251–272.
Zhang, R., Xu, X., 2009. Transient and transgenic analysis of the zebrafish ventricular myosin heavy chain (vmhc) promoter: an inhibitory mechanism of ventricle-specific gene expression. Dev. Dynam. 238, 1564–1573.
Zhang, Y., Liu, M., Liu, J., Wang, X., Wang, C., Ai, W., Chen, S., Wang, H., 2018. Combined toxicity of triclosan, 2,4-dichlorophenol and 2,4,6-trichlorophenol to zebrafish (*Danio rerio*). Environ. Toxicol. Pharmacol. 57, 9–18.
Zhong, W., Wang, D., Xu, X., Luo, Q., Wang, B., Shan, X., Wang, Z., 2010. Screening level ecological risk assessment for phenols in surface water of the Taihu Lake. Chemosphere 80, 998–1005.
Zhou, R., Xu, Q., Zheng, P., Yan, L., Zheng, J., Dai, G., 2008. Cardioprotective effect of fluvastatin on isoproterenol-induced myocardial infarction in rat. Eur. J. Pharmacol. 586, 244–250.